J Mater Sci: Mater Med (2011) 22:2803–2812
DOI 10.1007/s10856-011-4449-6

Conjugation of gold nanoparticles to polypropylene mesh for enhanced biocompatibility

D. N. Grant · J. Benson · M. J. Cozad · O. E. Whelove · S. L. Bachman · B. J. Ramshaw · D. A. Grant · S. A. Grant

Received: 20 April 2011 / Accepted: 23 September 2011 / Published online: 7 October 2011

Abstract Polypropylene mesh materials have been utilized in hernia surgery for over 40 years. However, they are prone to degradation due to the body's aggressive foreign body reaction, which may cause pain or complications, forcing mesh removal from the patient. To mitigate these complications, gold nanomaterials were attached to polypropylene mesh in order to improve cellular response. Pristine samples of polypropylene mesh were exposed to hydrogen peroxide/cobalt chloride solutions to induce formation of surface carboxyl functional groups. Gold nanoparticles were covalently linked to the mesh. Scanning electron microscopy confirmed the presence of gold nanoparticles. Differential scanning calorimetry and mechanical testing confirmed that the polypropylene did not undergo any significantly detrimental changes in physicochemical properties. A WST-1 cell culture study showed an increase in cellularity on the gold nanoparticle–polypropylene mesh as compared to pristine mesh. This study showed that biocompatibility of polypropylene mesh may be improved via the conjugation of gold nanoparticles.

1 Introduction

A hernia is described as a weakness or hole in the musculature resulting from a breakdown in the connective tissue or fascia covering the abdominal muscles. The weakness causes the muscular wall to become susceptible to protrusions of internal tissue or organs. The original method of hernia repair was a tension repair method in

D. N. Grant · J. Benson · O. E. Whelove
Department of Biological Engineering,
University of Missouri–Columbia, 162 Agricultural Engineering Building, Columbia, MO 65211, USA
e-mail: Dngcm8@mail.mizzou.edu

J. Benson
e-mail: Jrbm48@mail.mizzou.edu

O. E. Whelove
e-mail: oew9q7@mail.missouri.edu

M. J. Cozad
Department of Biological Engineering,
University of Missouri–Columbia, Room 148 Agricultural Engineering Building, Columbia, MO 65211, USA
e-mail: mjcozad@mizzou.edu

S. L. Bachman
Department of General Surgery,
University of Missouri–Columbia, Mc423 McHaney Hall, Columbia, MO 65211, USA
e-mail: bachmans@health.missouri.edu

B. J. Ramshaw
Department of General Surgery, Halifax Health,
Daytona Beach, FL, USA
e-mail: Bruce.Ramshaw@halifax.org

D. A. Grant
Department of Biological Engineering,
University of Missouri–Columbia, Room 210 Agricultural Engineering Building, Columbia, MO 65211, USA
e-mail: grantdav@missouri.edu

S. A. Grant (✉)
Department of Biological Engineering,
University of Missouri–Columbia, Room 250 Agricultural Engineering Building, Columbia, MO 65211, USA
e-mail: grantsa@missouri.edu

which the tissue surrounding the herniation was re-approximated and sutured to keep the protrusion contained. This primary repair method caused many complications, specifically recurrence, due to the tension occurring at the suture site in the already weakened tissue [1]. Because of this, tension-free repair using a synthetic mesh patch has become the standard in hernia repair surgeries with over one million implantations per year worldwide [1–5]. In 1958 Francis Usher introduced polypropylene hernia mesh which remains as one of the most widely used hernia repair materials today. Use of synthetic mesh patches, such as polypropylene, have been shown to be successful in hernia repair and reducing the risk for recurrence; however, the implantation of synthetic materials have also been found to elicit strong foreign body responses resulting in lack of biocompatibility and material inertness in vivo [4, 6].

Complications arising from polypropylene mesh may be due to its susceptibility to oxidation [7]. Costello et al. [8] reported that heavy weight polypropylene hernia mesh undergoes significant oxidation during its tenure in vivo. Others have reported shrinkage and migration problems with polypropylene mesh [9–12]. These complications limit the effectiveness and thus the performance of the material and, in some cases, require the removal of the mesh. Chemical surface treatments or modifications have been performed in order to enhance the biocompatibility of polypropylene. For example, functionalizing the polypropylene surface and/or changing its chemical properties may enhance biocompatibility according to Bhattacharyya et al. [13]. In another study, polypropylene was modified with star-configured polyethylene oxide based molecules [sP(EO-stat-PO)] and electrospun nanoweb of poly-lactide-co-glycolide with integrated sP(EO-stat-PO) [14]. Their in vivo results demonstrated good biocompatibility compared to the unmodified polypropylene mesh.

Another mechanism that has been investigated to improve biocompatibility is the conjugation of gold nanoparticles (AuNPs) to the polymer surface. For example, functionalizing poly(ether)urethane (PU) with AuNPs has been shown to reduce oxidation [15, 16]. After a 19 day in vivo pig study, histological analysis of explanted PU with AuNPs showed a significant reduction in the number of infiltrated inflammatory cells [16]. Macrophages and other phagocytes produce highly reactive oxygen species during inflammation that may initiate oxidation via free radicals. Thus, a reduction in inflammatory cells could decrease the oxidation of implants and thus improve the efficacy of the material. Additional benefits of incorporating AuNPs include enhancement of the antimicrobial properties of polymers [17]. Glass slides coated with AuNPs embedded in PP-g-PEG (polypropylene-polyethylene glycol) graft copolymers displayed significantly decreased numbers of bacteria colony forming units of *E. coli* and *S. aureus* [17].

Other studies have shown that proteins important for cell adhesion adsorb at higher concentrations on nanomaterials than on conventional materials [18]. Properties unique to nanomaterials such as increased surface energy due to increased grains at the surface may promote the adsorption of these proteins and lead to an improvement in cell adhesion. These properties may also lead to greater influence over subsequent cellular signaling cascades, differentiation, and gene expression [19–21]. Studies have shown that nanotopology/nanostructures can manipulate cellular behavior and it is well known that all biological systems are governed by molecular interactions at the nanometer length size [22–26]. For example, ECM (extracellular matrix) nanodots (100 nm^2) were utilized as focal adhesion points [22]. Nanoscale islands were also synthesized using poly dimethyl siloxane with heights varying from 10 to 100s of nm [27]. The researchers discovered that a nanoscale island height of $\sim$13 nm induced significant cell spreading and proliferation rates.

For this study, the surface of polypropylene mesh was chemically modified in order to conjugate amine-functionalized 20 nm gold nanoparticles for the purpose of enhancing surface biocompatibility. It was hypothesized that the addition of gold nanoparticles would result in increased cellularity without adversely altering the structural properties of the mesh.

2 Materials and methods

2.1 Materials

Polypropylene hernia mesh (Ultrapro™) was obtained from Ethicon (Somerville, NJ). Unconjugated 20 nm gold colloids were purchased from Ted Pella, Inc. (Redding, CA). *N*-hydroxysuccinimide (NHS) was obtained through Pierce, a division of Thermo Fisher Scientific (Rockford, IL). Cobalt chloride ($CoCl_2$), 2-mercaptoethylamine (MEA), 1-ethyl-3-[3-dimethylaminopropyl]carbodiimide hydrochloride (EDC), acetone, phosphate buffer (PBS), and hydrogen peroxide (H_2O_2) were obtained from Sigma-Aldrich (St. Louis, MO). L-929 murine fibroblasts (CCL-1), culture medium (Eagle's Minimum Essential Medium, horse serum, penicillin–streptomycin), and Dulbecco's Phosphate Buffered Saline (DPBS) were purchased from American Type Culture Collection (ATCC, Manassas, VA). The water soluble tetrazolium (WST-1) reagent was purchased through Roche Diagnostics (Indianapolis, IN).

2.2 Material preparation

Seven pristine polypropylene mesh pieces were cut into rectangles approximately 4 × 10 cm. The samples were

placed into 200 ml beakers of distilled/deionized water (ddH_2O) and boiled for approximately 10 min to clean the surface. Once the boiling process was complete the samples were dried in a desiccator for 2 days. After being thoroughly dried, FT-IR spectra were obtained for each of the pristine polypropylene samples. Next, six of the mesh pieces were exposed to the cobalt chloride/hydrogen peroxide solution. Of the six mesh pieces, three of the mesh were further conjugation to gold nanoparticles as described in the following sections.

2.3 Cobalt chloride/hydrogen peroxide treatment

Following a procedure similar to Christenson et al. [28], a hydrogen peroxide solution containing cobalt chloride was prepared by combining 50 ml ddH_2O, 50 ml of 50% (v/v) H_2O_2 and 1.29 mg of $CoCl_2$ ($\sim$0.2 mM). This $CoCl_2/H_2O_2$ solution was then added to a 200 ml Erlenmeyer flask containing a polypropylene mesh to promote formation of carboxyl functional groups on the surface of the mesh (one mesh per flask). The flask was placed on a shaker table set at 150 rpm for 72 h. After this time, the samples were removed, rinsed in ddH_2O and allowed to dry for 2 days. FT-IR scans were then obtained to determine the presence of carboxyl groups, which will be utilized to promote bonding to the amine functionalized AuNPs. It was desirable to functionalize the surface with carboxyl groups in order to provide attachment sites for the AuNPs. However, the process to achieve this is an oxidation process (free radical generation) and thus has the possibility of affecting the mechanical properties of the mesh. To ascertain that this process avoids adverse effects on the mesh, characterization studies were performed as described in Sect. 2.5.

2.4 Gold nanoparticle crosslinking treatment

A crosslinking procedure was developed in order to attach the 20 nm diameter AuNPs to the surface of the polypropylene material [29, 30]. Gold nanoparticles were first coated with 2-mercaptoethylamine (MEA) in order to functionalize them with amine groups to promote covalent bonding to the chemically modified polypropylene. The optimal concentration of MEA was previously determined through the use of UV–Vis spectroscopy before and after the addition of an electrolyte (10% NaCl) [29, 30]. The optimal concentration was defined as the concentration of MEA that stabilized the AuNPs, preventing aggregation and maintaining dispersion even after the addition of 10% NaCl [31]. Ultimately, functionalization of the AuNPs in this study was performed by mixing 500 µl of the aqueous gold colloid solution (pH 5.5) with 50 µl of concentrated (15 µM) MEA solution.

The crosslinking solution consisted of a 50:50 (v/v) solution of acetone and PBS (pH 7.5) with a final concentration of 5 mM NHS and 2 mM EDC, a non-toxic, zero-length crosslinker. Because it is a "zero-length" crosslinker, EDC does not become part of the crosslink. For this reason, there is very little threat of a cytotoxic reaction since none of the crosslinking chemicals remain within the mesh [32].

Three of the mesh pieces were conjugated to AuNPs. The $CoCl_2/H_2O_2$ treated polypropylene samples were placed in individual 100 ml of crosslinking solution for 20 min. After 20 min, the crosslinking solution was removed from the individual polypropylene samples. Then the functionalized AuNP solution ($\sim$10 ml) was added to completely cover the material surface and the samples were stirred via an orbital shaker table for 20 min. The concentration of the AuNPs was 7×10^{11} particles/ml. The solution was then removed and replaced with PBS, where it was stirred via an orbital shaker table for 24 h in order to rinse the materials. After 24 h, the PBS was then removed and the samples were allowed to dry for 2 days. The mesh pieces were then cut to size for the characterization studies.

2.5 Characterization

2.5.1 Morphology

Scanning electron microscopy (SEM) and energy dispersive spectroscopy (EDS) were performed to determine if the AuNPs were attached to the surface of the modified polypropylene samples. Micrographs of the samples were obtained using a field emission scanning electron microscope (Quanta™ 600, FEI Company, Hillsboro, OR) and an energy dispersive spectroscopy (EDS) system (Thermo Scientific NORAN System Six, Thermo Fisher Scientific, Waltham, MA). These micrographs were analyzed with the NIH image software program, ImageJ, to determine the average AuNP density on the polypropylene specimens [33]. Four AuNP–PP samples and one pristine sample were analyzed, and no preparation of the mesh was necessary prior to SEM imaging.

2.5.2 Surface chemical characterization

A Nicolet 6700 FT-IR spectrometer (Thermo Scientific, Waltham, MA) was utilized to collect spectra by averaging 32 scans with a resolution of 4/cm at ambient temperature to determine the presence of carboxyl and carbonyls groups (1,740 and 1,350/cm range). These peaks would indicate functional groups, which will allow conjugation of the functionalized AuNPs. The ATR (attenuated total reflectance) crystal was utilized in order to perform surface scans, which have a penetration depth of 2–4 µm. Three separate locations were scanned for each specimen. Three specimens of pristine were scanned and three specimens of

the chemically-treated polypropylene were scanned. FT-IR scans were performed in order to make a comparison between the polypropylene mesh samples to note the addition of new functional groups to the material surface.

2.5.3 Mechanical characterization

A standard uniaxial tensile test was performed on five pieces of each of the pristine polypropylene and chemically modified polypropylene in order to determine if any changes in mechanical strength occurred. The mesh was cut down to a 2 × 10 cm size and a v-shaped notch was cut into both sides of the central region of each specimen to reduce the width by 40%. The intent was to create a stress concentration at the center of the specimen and prevent a failure of the mesh in the grip. A template was utilized to prepare each specimen to ensure the reproducibility of these notches, and the thickness of each specimen was measured using digital calipers prior to uniaxial tensile testing. The specimens were gripped 10 mm at each end with pneumatic grips set to 52 psi and an Instron 5864 Universal Testing Machine (Norwood, MA) was utilized to strain the specimens at a rate of 0.2 mm/s until failure. All specimens were strained in the direction parallel to the major weave direction of the polypropylene mesh. The ratio of the grip-to-grip length versus the reduced width at the center of the specimen was 4:1. Instron Bluehill software was utilized to calculate the mechanical properties. The tensile stress at maximum load and Young's modulus were determined for both the pristine and chemically-treated polypropylene specimens.

2.5.4 Thermal characterization

The samples were subjected to modulated differential scanning calorimetry (DSC) using a Q2000 DSC (TA Instruments, New Castle, DE) to ramp the temperature from −90 to 220°C at a rate of 5°C per min with a modulation of ±0.64°C every 80 s. The total heat flow signal was analyzed to obtain the heat of fusion, onset temperature, and melt temperature. Six specimens of AuNP–polypropylene and six specimens of the pristine polypropylene were cut into 3 mm by 3 mm squares. Each specimen was placed in an aluminum pan and sealed with a hermetic lid. The heat of fusion, onset temperature, and melt temperatures of the AuNP–polypropylene specimens were analyzed and compared to the pristine polypropylene to determine if the materials thermal properties were adversely altered by the $CoCl_2/H_2O_2$ chemical treatment. The thermal properties are not expected to change; however, the presence of AuNPs may influence the heat of fusion due to the heat absorption by the gold nanoparticles.

2.5.5 Seven day WST-1 assay study

A 7 day WST-1 cell culture assay study was performed in order to examine the response of the L-929 cells to the AuNP–polypropylene as compared to the pristine polypropylene. This colorimetric assay allows for the assessment of the cellularity of the culture exposed to the specimens as well as the cytotoxicity of the AuNPs. Specifically, the WST-1 assay involves the cleavage of tetrazolium salts into formazan via mitochondrial dehydrogenases. Absorbance measurements at 450 nm with a Model 680 Microplate Reader (Bio-Rad Laboratories, Philadelphia, PA) indicate the levels of formazan in the cell culture and thus, the number of metabolically active cells in the culture. Cell culture medium with the WST-1 assay reagent, but without cells, was used as a blank.

L-929 murine fibroblast cells were cultured in Eagle's minimum essential medium supplemented with 10% horse serum and 200 units/ml penicillin–streptomycin. The cells were incubated at 37°C under a 5% CO_2 atmosphere. When the cells in the culture flask reached approximately 80% confluency, they were subcultured. To subculture, the cells were trypsinized, centrifuged, and then re-suspended in sterile culture medium. To avoid deviations, the passage numbers of cells utilized in these studies ranged from 30 to 40.

Six pristine polypropylene specimens and six AuNP–polypropylene specimens were cut to a size of 5 mm by 5 mm. All specimens were autoclaved for 35 min at 121°C prior to being placed into individual wells of a 24-well culture plate in a non-random order. To each well containing AuNP–polypropylene mesh and pristine polypropylene mesh, 1 ml of cell suspension with a cell concentration of 1.5×10^4 cells/ml was added. A blank was also created that contained no mesh, only culture medium. The well plate was covered and then placed in the incubator at 37°C and 5% CO_2 for 7 days. To assure proper cell growth, the culture medium was changed on the third and fifth days of the assay by carefully removing 0.5 ml of medium from each well and replacing with 0.5 ml of fresh culture medium.

After 7 days of incubation, 0.5 ml of media was withdrawn from each well and WST-1 reagent was added at a 1:10 ratio of WST-1 to culture suspension and again incubated for 1 h at 37°C and 5% CO_2. Then the 24-well plate was removed from the incubator and 100 μl of solution from each scaffold well and the blank was transferred to a well in a 96-well microplate. The formazan dye produced from the reduction of WST-1 by viable cells was measured by reading the absorbance with a microplate reader. The number of viable cells was correlated to the absorbance measurements by subtracting the blank absorbance from the raw absorbance values to account for any absorbance encountered from the culture medium.

2.6 Statistics

Statistical analyses were carried out using GraphPad Prism version 4.0 (GraphPad Software, Inc., San Diego, CA). A one-way ANOVA was performed, followed by a Tukey all pair-wise multiple comparison test with significance set at $P < 0.05$.

3 Results

3.1 FT-IR analysis of polypropylene surface

Figure 1 displays a representative FT-IR scan of a pristine polypropylene specimen and an FT-IR scan of $CoCl_2/H_2O_2$ treated polypropylene specimen. The results showed that the solution was capable of modifying the polypropylene surface by introducing functional groups to the surface; thus, providing conjugation sites for the amine-functionalized AuNPs. There are noticeable peaks around the 1,740 and 1,350/cm range for the $CoCl_2/H_2O_2$ treated polypropylene that are not prominent in the pristine mesh. These specific changes demonstrate the addition of functional groups such as carbonyls and carboxyl groups on the material surface, which will allow conjugation of the functionalized AuNPs. Reproducible results were obtained with all of the $CoCl_2/H_2O_2$ treated specimens.

3.2 SEM characterization

SEM was utilized to determine if the AuNPs were immobilized onto the polypropylene surface and if so, at what surface density. Also, it was desirable to determine if the surface of the material underwent adverse morphology changes such as pitting and/or cracking due to the $CoCl_2/H_2O_2$ chemical treatment. The EDS allowed for the determination of the composition of the immobilized particles to ascertain that they were AuNPs.

Figure 2a displays an SEM micrograph of a pristine polypropylene mesh while Fig. 2b displays a $CoCl_2/H_2O_2$ treated polypropylene. At 913× magnification, agglomerations of AuNPs appear etched onto the surface of the polypropylene fibers. Also, the longitudinal extrusion lines of the individual polypropylene fibers are seen. At a higher magnification as shown in Fig. 2c, it does not appear as if the fibers suffered any cracking or pitting. It appears as if the AuNPs are covalently attached to the surface in small to large agglomerations. As determined from Image J software analysis, the AuNPs covered an area of $\sim$26.4 μm^2 on the mesh surface totaling 764.5 μm^2 This equals a surface coverage of 3.45% or 0.0345 μm^2 of AuNPs per square micrometer of mesh. Four SEM mesh micrographs were analyzed and the results were averaged.

To determine the composition of the agglomerations, EDS was utilized. Four different targets were selected for analysis as shown in Fig. 2d. The fourth target was a blank target for control. Targets 1 through 3 demonstrated the presence of gold as noted in the EDS scan shown in Fig. 2e along with the presence of the carbon (C) peaks and the oxygen (O) peaks, which are representative of the chemically treated polypropylene material. Target 4, the control target, only demonstrated the presence of the carbon and oxygen peaks, as expected.

3.3 Mechanical analysis results

The results of the uniaxial tensile test are depicted in Fig. 3 in which the mean tensile stress at maximum load

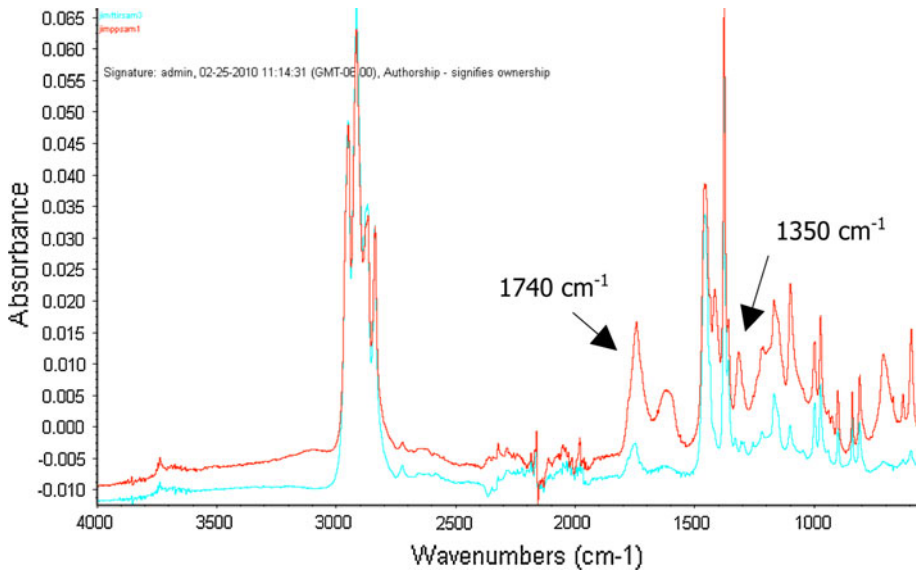

Fig. 1 FT-IR spectra of pristine polypropylene (*blue*) and AuNP–polypropylene meshes (*red*). There is carbonyl formation near 1,740/cm

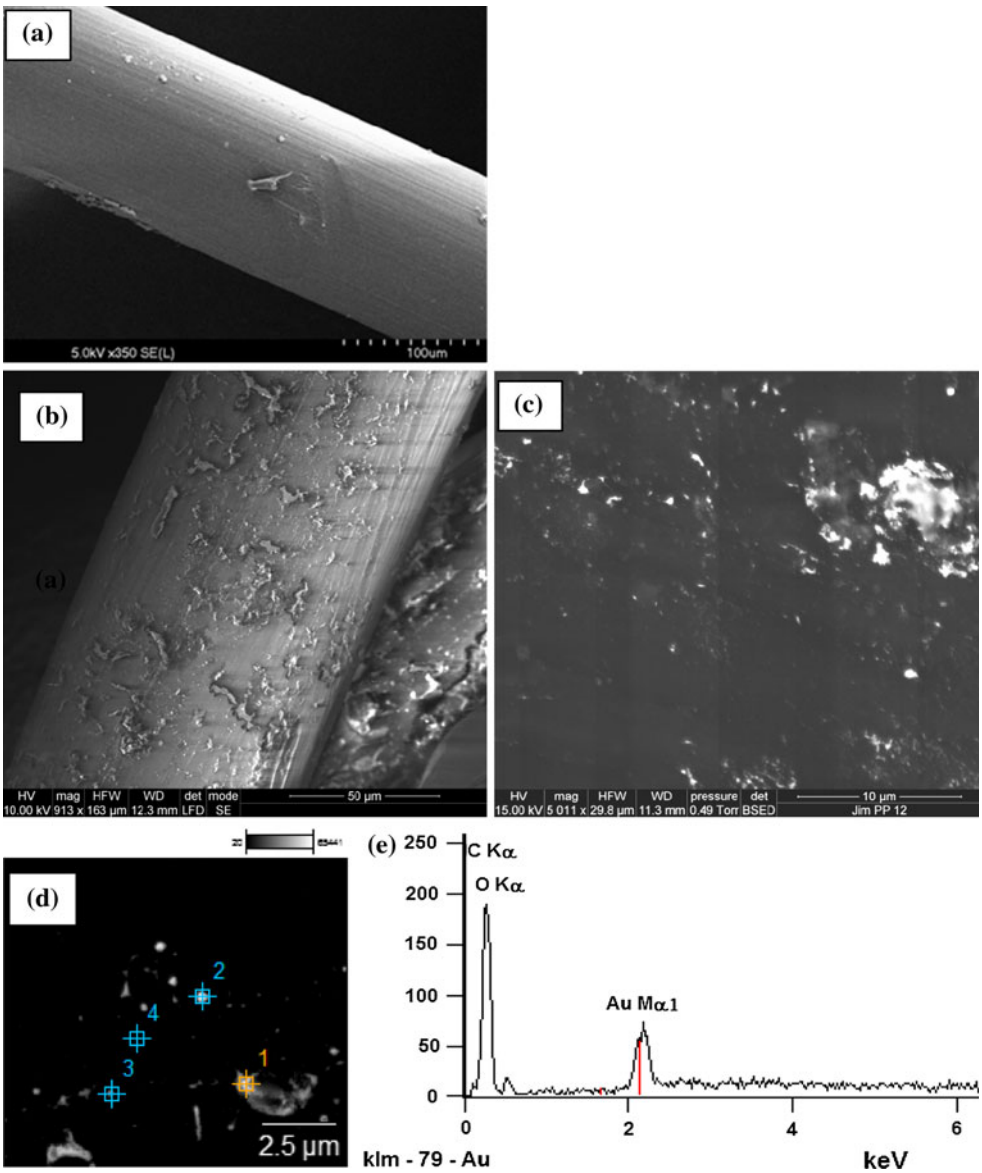

Fig. 2 **a** Secondary electron SEM image of a pristine polypropylene mesh [working distance of 12.3 mm, and a chamber pressure of 0.45 Torr. (*scale bar* 100 mm)]; **b** Secondary electron SEM image of AuNP–polypropylene mesh showing distribution of particles along the surface [working distance of 12.3 mm, and a chamber pressure of 0.45 Torr (*scale bar* 50 µm)]; **c** Back-scatter SEM image of AuNP–polypropylene mesh showing charged particles of various sizes scattered across the surface [working distance of 11.3 mm, and a chamber pressure of 0.49 Torr (*scale bar* 10 µm)]; **d** Surface image of polypropylene using SEM with points selected for composition analysis using EDS. **e** EDS analysis of point 2 (from Fig. 2c) on the surface. Points 1–3 all showed similar results

is plotted ± the standard error. The pristine specimens displayed a mean tensile stress of 16.59 ± 1.08 MPa while the mean tensile stress of the chemically-treated polypropylene specimens was 18.13 ± 2.59 MPa. There was no significant difference ($P = 0.5745$) in tensile stress at maximum load indicating that the $CoCl_2/H_2O_2$ chemical treatment did not adversely affect the polypropylene specimens. The Young's modulus of the specimens was also determined as noted in Fig. 4. The pristine specimens displayed a significantly higher modulus ($P = 0.0202$) than the chemically treated-polypropylene specimens. The pristine specimen display a mean modulus of 123.5 ± 6.98 MPa while the mean modulus of the chemically treated-polypropylene specimens was 84.42 ± 12.8 MPa.

3.4 Thermal analysis results

DSC was utilized to analyze the thermal transitions of the AuNP–polypropylene specimens. These results were then compared with pristine specimens. Table 1 displays the onset temperature, melt temperature, and heat of fusion for the AuNP–polypropylene specimens as compared to the pristine specimens. The mean onset and melt temperatures are reported in units of °C ± standard error while heat of fusion is reported in units of J/g ± standard error. Results from the pristine specimens were similar to the AuNP–polypropylene specimens for onset and melt temperatures and thus these values were not significantly different. The mean onset temperature ± standard error for pristine and AuNP–polypropylene specimens were similar with

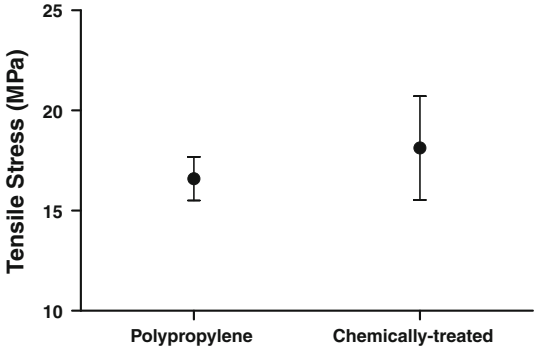

Fig. 3 Uniaxial testing results showing tensile stress at maximum load for pristine and chemically treated-polypropylene mesh

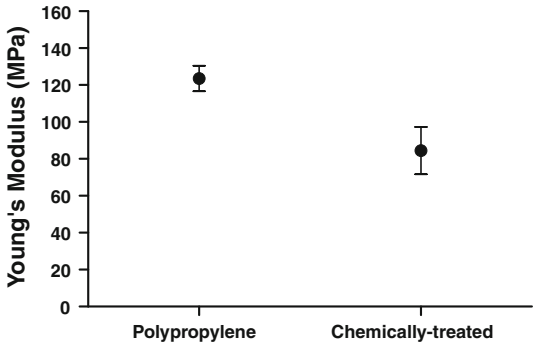

Fig. 4 Uniaxial testing results showing modulus of elasticity for pristine and chemically treated-polypropylene mesh

160.0 ± 1.159°C and 157.8 ± 1.088°C ($P = 0.9955$), respectively. The mean melt temperature ± standard error for pristine and AuNP–polypropylene specimens were 166.9 ± 0.7814°C and 167.8 ± 0.4528°C ($P = 0.2139$), respectively. However, AuNP–polypropylene specimens resulted in a significant increase ($P = 0.0036$) in heat of fusion relative to pristine specimens with 37.34 ± 2.681 and 14.83 ± 4.851 J/g, respectively.

3.5 Cellularity results

Cellularity of L-929 fibroblasts and cytotoxicity of AuNPs conjugated to polypropylene mesh were simultaneously assessed using the WST-1 assay. Absorbance readings were obtained after 1 h incubation of WST-1 reagent with the 7 day cell/scaffold culture and are summarized in Fig. 5. It can be seen from the graph that much higher absorbance values were measured for the AuNP–polypropylene specimens, whereas the pristine polypropylene specimens showed significantly lower absorbance values ($P = 0.0117$).

4 Discussion

For over 40 years, polypropylene (mono-filament polypropylene and dual filament polypropylene) has been the predominant mesh used for hernia repair [1]. For hernia mesh, semi-crystalline polypropylene fibers are extruded and then are woven into particular monofilament or multi-filament mesh designs. Unfortunately, polypropylene mesh has been shown to oxidize and degrade in vivo [34]. Oxidation occurs when the C–H bonds are compromised; creating a free radical that will bind with oxygen. Chain scission and/or crosslinking may occur and this "embrittlement" may change the physicochemical properties of the polypropylene. For example, polypropylene mesh may become stiff and/or can shrink, which can result in pain or recurrence of the hernia in some patients. To improve the overall efficacy of the polypropylene mesh, gold nanoparticles were conjugated to the surface and then characterized.

Previous studies have demonstrated the ability of AuNPs to act as free radical scavengers [15, 16]. During an inflammatory response, highly reactive oxygen species, such as free radicals, are produced by the phagocytes, which can lead to oxidation of the polypropylene material. Gold nanoparticles are electron deficient therefore they will bind with extra electrons. Thus, the capture of free radicals by the AuNPs can reduce the incidences of oxidation of the mesh material during their tenure in vivo.

SEM images demonstrated the presence of the AuNPs on the polypropylene surface while also providing visualization of the surface structure of the modified polypropylene fibers. The charged AuNPs are abundant on the AuNP–polypropylene scaffold surfaces as seen in Fig. 2b suggesting successful crosslinking of the amine-functionalized AuNPs to the carboxyl groups. Image analysis demonstrated 3.45% coverage of AuNPs on the surface as well. The presence of AuNPs was confirmed via elemental analysis with EDS, which displayed a surface composition scan of carbon, oxygen, and gold peaks.

The SEM micrographs also displayed some interesting surface morphology. The surface was analyzed for

Table 1 Results of onset temperature, melt temperature, and heat of fusion of the pristine and AuNP–polypropylene mesh

Specimen	Onset temperature (°C)	Melt temperature (°C)	Heat of fusion (J/g)
Polypropylene	160.0 ± 1.159	166.9 ± 0.7814	14.83 ± 4.851
AuNP–polypropylene	157.8 ± 1.088	167.8 ± 0.4528	37.34 ± 2.681

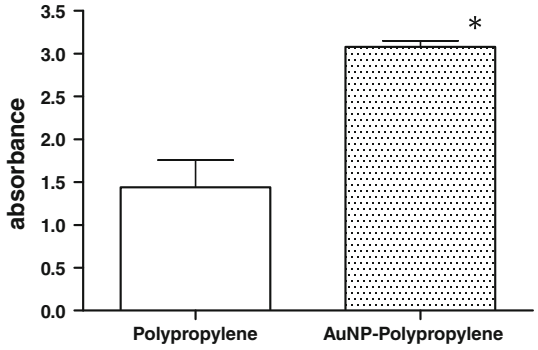

Fig. 5 Absorbance values obtained with the WST-1 assay for the pristine polypropylene and AuNP–polypropylene mesh following a 7 day cell culture and 2 h incubation with the WST-1 reagent. * Indicates mean significantly higher than the pristine ($P = 0.0117$)

evidence of degradation due to the $CoCl_2/H_2O_2$ treatment. No obvious stress cracking or breaks in the polypropylene fibers were found; however, it appeared as if the AuNPs had a tendency to agglomerate. In the low magnification image, a polypropylene fiber is visible that contains ~20 um long AuNPs "ribbons" that are scattered throughout the surface of the fiber. Upon higher magnification, AuNP clumps are evident as well as smaller, scattered AuNPs. Because of this unusual surface morphology, uniaxial testing and thermal testing were performed to ascertain any changes in the polypropylene's physiochemical structure.

The primary goal of synthetic hernia mesh is to provide mechanical support in order to prevent hernia recurrence. For example, an important criterion is that the mesh must have the necessary tensile strength to withstand the maximum intra-abdominal forces, which is estimated to be approximately 170 mmHg (~22 kPa) during coughing [35]. While current commercial meshes possess very high tensile strength and burst pressures, they are potentially over engineered for most people. In this study, the tensile stress at maximum load for the chemically treated AuNP–polypropylene mesh was not statistically difference from the pristine. Both types of mesh demonstrated high tensile stress, indicating that the chemically-treated mesh, as well as the pristine, have more than sufficient strength to withstand intra-abdominal forces. However, the elastic modulus of the pristine mesh was significantly different from the chemically-treated mesh. The pristine mesh displayed a higher modulus while the chemically treated mesh was more compliant. It is unclear why the chemically-treated mesh had a lower modulus while maintaining the high tensile strength. One reason could be that the chemical treatment allowed rearrangement or displacement of the polymeric chains resulting in a more compliant property of the material structure. This could be considered evidence of mesh damage; however, possessing more compliancy while maintaining strength may result in better overall biocompatibility. For instance, the optimal stiffness of a hernia repair material would be one that matches the tissue properties. By having a more compliant mesh or better matched mesh, it is possible that there may be less inflammatory response and better integration of the surrounding tissue. However, a hernia mesh that is too compliant could result in recurrence of the hernia.

Analysis of the thermal properties demonstrated that the onset and melt temperatures for the pristine and chemically-treated mesh were not significantly different. Interestingly, the heat of fusion was significantly higher for the chemically-treated mesh. This may be due to the gold nanoparticles, which can absorb energy, causing the heat of fusion to be higher. As a precaution, DSC scans were repeated on just the chemically-treated mesh without AuNPs. The results showed that the heat of fusion was not significantly different from pristine, indicating that the presence of AuNPs caused an increase in the heat of fusion. Therefore, our analysis of chemically-treated polypropylene and the pristine mesh demonstrated no significant differences in onset temperature, melt temperature, or heat of fusion, suggesting that the bulk material properties were retained during the chemical treatment procedures.

The mesh surface properties and interactions with the surrounding tissues will define its biocompatibility and long-term efficacy [36]. There are many assays kits available that can test the cytotoxicity or the biocompatibility of a material, such as MTT assays, direct contact assays, and WST-1 assays. The results from the WST-1 assays performed in this study demonstrated a significant increase in absorbance in solutions exposed to the AuNP–polypropylene mesh as compared to the pristine polypropylene. The WST-1 assay is based on the reduction of tetrazolium to formazan dye which occurs due to the metabolic activity in viable cells. The amount of formazan dye produced is measured by a UV/Vis spectrometer, and thus, greater amounts of formazan dye correlate to higher metabolic activity of the cells during incubation. This then correlates to enhanced cellularity. Based on the results of the WST-1 assay, polypropylene mesh conjugated to gold nanoparticles demonstrated significantly greater viability of L-929 fibroblasts over pristine polypropylene mesh.

5 Conclusion

The results obtained from this study demonstrated that conjugation of gold nanoparticles to chemically-modified polypropylene mesh increased the cellularity without adversely affecting the structural properties. The FT-IR

results demonstrated successful chemical treatments, which generated new functional groups on the surface. Uniaxial tensile testing and DSC results demonstrated that the $CoCl_2/H_2O_2$ chemical treatment did not adversely affect its physicochemical properties and may improve the interface between tissue and mesh via a reduction in mesh stiffness. A cell culture assay, WST-1, demonstrated the effectiveness of the AuNPs to increase cellularity. Attaching gold nanoparticles to mesh scaffolds may be a viable option for improving the efficacy of polypropylene hernia mesh.

Acknowledgments The authors would like to acknowledge funding from the Missouri F21C Food for the 21st Century.

References

1. Brown CN, Finch JG. Which mesh for hernia repair? Ann R Coll Surg Engl. 2010;92(4):272–8.
2. Bringman S, Conze J, Cuccurullo D, Deprest J, Junge K, Klosterhalfen B, Parra-Davila E, Ramshaw B, Schumpelick V. Hernia repair: the search for ideal meshes. Hernia. 2010;14(1):81–7.
3. Yang J, Papandria D, Rhee D, Perry H, Abdullah F. Low-cost mesh for inguinal hernia repair in resource-limited settings. Hernia. 2011; In press.
4. Voskerician G, Jin J, White M, Williams C, Rosen M. Effect of biomaterial design criteria on the performance of surgical meshes for abdominal hernia repair: a pre-clinical evaluation in a chronic rat model. J Mater Sci Mater Med. 2010;21(6):1989–95.
5. Nelson EC, Vidovszky TJ. Composite mesh migration into the sigmoid colon following ventral hernia repair. Hernia. 2011; 15(1):47–52.
6. Cozad MJ, Ramshaw BR, Grant DN, Bachman SL, Grant DA, Grant SA. Materials characterization of explanted polypropylene, polyethylene terephthalate, and expanded polytetrafluoroethylene composites: spectral and thermal analysis. J Biomed Mater Res B. 2010;49B:455–62.
7. Sutherland K, Mahoney JR, Coury AJ, Eaton JW. Degradation of biomaterials by phagocyte-derived oxidants. J Clin Invest. 1993;92:2360–7.
8. Costello CR, Bachman SL, Ramshaw BR, Grant SA. Materials characterization of explanted heavyweight polypropylene hernia meshes. J Biomed Mater Res B. 2007;83B:44–9.
9. Zinther NB, Wara P, Friis-Andersen H. Shrinkage of intraperitoneal onlay mesh in sheep: coated polyester mesh versus covered polypropylene mesh. Hernia. 2010;14(6):611–5.
10. Beldi G, Wagner M, Bruegger LE, Kurmann A, Candinas D. Mesh shrinkage and pain in laparoscopic ventral hernia repair: a randomized clinical trial comparing suture versus tack mesh fixation. Surg Endosc. 2010;24(6):1451–5.
11. Khan RN, Kindal V, Bansal VK, Misra MC, Kumar S. Does mesh shrinkage in any way depend upon the method of mesh fixation in laparoscopic incisional hernia repair? Surgical Endoscopy. 2010. doi:10.1007/s00464-010-1363-9.
12. Downey DM, Dubose JJ, Ritter TA, Dolan JP. Validation of a radiographic model for the assessment of mesh migration. J Surg Res. 2011;166:109–13.
13. Bhattacharyya AR, Sreekumar TV, Liu T, Kumar S, Ericson LM, Hauge RH, Smalley RE. Crystallization and orientation studies in polypropylene/single wall carbon nanotube composite. Polymers. 2003;44(8):2373–7.
14. Bohm, G, Ushakova Y, Alizai H, Braunschweig T, Lente C, Heffels K, Groll J, Neumann U, Junge D. Biocompatibility of PLGA/sP(EO-stat-PO)-coated mesh surfaces under constant shearing stress. Eur Surg Res. 2011;47(3):118–129.
15. Hsu S, Tang C, Tseng H. Biocompatibility of poly(ether)urethane-gold nanocomposites. J Biomed Mater Res A. 2006;79: 759–70.
16. Chou C, Hsu S, Wang P. Biostability and biocompatibility of poly(ether)urethane containing gold or silver nanoparticles in a porcine model. J Biomed Mater Res A. 2007;84:785–94.
17. Kalayci O, Comert F, Hazer B, Atalay T, Cavicchi K, Cakmak M. Synthesis, characterization, and antibacterial activity of metal nanoparticles embedded into amphiphilic comb-type graft copolymers. Polym Bull. 2010;65:215–26.
18. Christenson EM, Anseth KS, van den Beucken LJ, Chan CK, Ercan B, Jansen JA, Laurencin CT, Li WJ, Murugan R, Nair LS. Nanobiomaterial applications in orthopedics. J Orthop Res. 2007;25:11–22.
19. Balasundaram G, Webster TJ. A perspective on nanophase materials for orthopedic implant applications. J Mater Chem. 2006;16:3737–45.
20. Dillow AK, Lowman AM. Biomimetic materials and design. New York: Marcel Dekker Inc.; 2002.
21. Kay S, Thapa A, Haberstroh KM, Webster TJ. Nanostructured polymer/nanophase ceramic composites enhance osteoblast and chondrocyte adhesion. Tissue Eng. 2002;8:753–61.
22. Sniakecki NJ, Desai RA, Ruiz SA, Chen CS. Nanotechnology for cell-substrate interactions. Ann Biomed Eng. 2006;34(1): 59–74.
23. Teixeira AI, Nealey PF, Murphy CJ. Responses of human keratocytes to micro-nanostructured substrates. J Biomed Mater Res. 2004;71A:3153–64.
24. Yim EK, Reano RM, Pang SW, Yee AF, Chen CS, Leong KW. Nanopattern-induced changes in morphology and motility of smooth muscle cells. Biomaterials. 2005;26:5405–13.
25. Curtis AS, Wilkinson CD, Crossan J, Broadley C, Darmani H, Johal KK, Jorgensen H, Monaghan W. An in vivo microfabricated scaffold for tendon repair. Eur Cell Mater. 2005;9: 50–7.
26. Foley JD, Grunwald E, Nealey PF, Murphy CJ. Cooperative modulation of neuritogenesis by PC12 cells by topography and nerve growth factor. Biomaterials. 2005;26:3639–44.
27. Dalby MJ, Yarwood SJ, Riehle MO, Johnstone HJ, Affrossman S, Curtis AS. Increasing fibroblast response to materials using nanotopogrpahy: Morphological and genetic measurements of cell response to 13-nm-high- polymer demixed islands. Exp Cell Res. 2002;276:2002.
28. Christenson EM, Anderson JM, Hiltner A. Oxidative mechanisms of poly(carbonate urethane) and poly(ether urethane) biodegradation: In vivo and in vitro correlations. J Biomed Mat Res A. 2004;70(2):245–55.
29. Deeken CR, Fox DB, Bachman SL, Ramshaw BJ, Grant SA. Characterization of bionanocomposite scaffolds comprised of amine-functionalized gold nanoparticles and silicon carbide nanowires crosslinked to an acellular porcine tendon. J Biomed Mater Res B. 2011;99(1):142–9.
30. Deeken CR, Fox DB, Bachman SL, Ramshaw BJ, Grant SA. Assessment of the biocompatibility of two novel, bionanocomposite scaffolds in a rodent model. J Biomed Mater Res B. 2011;96B(2):351–9.
31. Hermanson G. Preparation of colloidal-gold-labeled proteins, bioconjugate techniques. New York: Academic Press; 1996.
32. Badylak SF, Lantz GC, Coffey A, Geddes LA. Small intestinal submucosa as a large diameter vascular graft in the dog. J Surg Res. 1989;47:74–80.
33. http://rsbweb.nih.gov/ij/download.html.

34. Costello CR, Bachman SL, Grant SA, Cleveland DS, Loy TS, Ramshaw BR. Characterization of heavyweight and lightweight polypropylene prosthetic mesh explants from a single patient. Surg Innov. 2007;14(3):168–76.
35. Cobb WS, Burns JM, Kercher KW, Matthews BD, Norton HJ, Heniford BT. Normal intraabdominal pressure in healthy adults. J Surg Res. 2005;129:231–5.
36. Emans P, Schreinemacher M, Gijbels M, Beets G, Greve J-W, Koole L, Bouvy N. Polypropylene meshes to prevent abdominal herniation can stable coatings prevent adhesions in the long term? Ann Biomed Eng. 2009;37(2):410–8.